Adsorptive and DFT Studies of Some Imidazolium Based Ionic Liquids as Corrosion Inhibitors for Zinc in Acidic Medium

Kgabo M. Manamela[1], Lutendo C. Murulana[1,2,*], Mwadham M. Kabanda[2], Eno. E. Ebenso[2]

[1] Department of Chemistry, School of Mineral and Physical Sciences, University of Limpopo, Turfloop Campus, Private Bag X 1106, Sovenga 0727, South Africa
[2] Material Science Innovation & Modelling (MaSIM) Research Focus Area, Faculty of Agriculture, Science and Technology, North-West University (Mafikeng Campus), Private Bag X2046, Mmabatho, 2735, South Africa
[*]E-mail: lutendo.murulana@ul.ac.za

The corrosion inhibition ability of 1-butyl-3-methylimidazolium tetrafluoroborate [BMIM][BF_4^-] and 1-decyl-3-methylimidazolium tetrafluoroborate [DMIM][BF_4^-] ionic liquids (ILs) on zinc surface in 1.0 M HCl at 30 - 50°C was investigated using gravimetric analysis and theoretical Density Functional Theory (DFT) approach, using the B3LYP functional. Thermodynamic and kinetic parameters such as ΔG^o_{ads}, E_a, ΔS^*, ΔH^* were calculated. The adsorption of ILs on zinc surface adopted the Langmuir adsorption isotherm model. The values of E_a and ΔH^* suggested a physisorption process. Both experimental and theoretical results show that the two ionic liquids are good corrosion inhibitors for zinc corrosion in 1.0 M HCl solutions and their inhibition efficiency follows the order: [DMIM][BF_4^-] > [BMIM][BF_4^-].

1. INTRODUCTION

The corrosion phenomenon of materials has been of a major concern for a long time to many industries due to its consequences on industrial equipments such as reaction vessels, engineering vehicles, mining equipments and packaging machineries. The other major challenge associated with corrosion is the contamination of industrial products [1]. Corrosion mostly involves the deterioration of the materials and it is widely common in metals although it is not limited to them. Materials of different types such as plastics, ceramics and composites are also prone to the wrath of corrosion. The effects of corrosion are detrimental to humans. These effects do not only badly damage the economy of a particular nation but also have a tremendous negative impact on human health. The importance of

studying zinc corrosion is related to the fact that various zinc metals have several industrial applications. The exposure of zinc metals to harsh conditions, such as low and high pH environments usually found in petroleum or chemical industries, may lead to the corrosion of these metals, thereby losing their mechanical properties. This loss causes metals to compromise on their optimum performance. The need to protect zinc metals from corroding has lead to many scientific investigations [2-6]. Organic compounds containing electronegative functional groups and π-electrons in triple or conjugated double bonds are usually good corrosion inhibitors. Heteroatoms such as sulphur (S), phosphorus (P), nitrogen (N) and oxygen (O) as well as aromatic rings in their structure are the major adsorption centers [7-12]. Corrosion inhibitors facilitate in the retardation of zinc corrosion through the formation of adsorption films between zinc surface and the compound of interest. The mechanism of formation of these adsorption films may be classified as physisorption, chemisorption or a combination of the two, that is, mixed type. Physisorption or physical adsorption is associated with the electrostatic interactions between charged metal and charged molecules, while chemisorption or chemical adsorption is associated with the formation of a covalent bond resulting from the charge sharing or transfer from corrosion inhibitor molecules to the metal surface [12]. The strength and stability of the formed adsorption layer depends entirely on the type of the metal, the nature of the corrosion inhibitor, the type of interaction that exist between the d-orbital of the zinc metal and the π-orbital of the corrosion inhibitor, steric effects and the nature of the corrosive medium [13]. Current investigations reveal that the use of corrosion inhibitors that evidently carry minimal or zero toxicity while exhibiting good inhibition efficiency is advantageous [14].

[BMIM][BF$_4^-$]   [DMIM][BF$_4^-$]
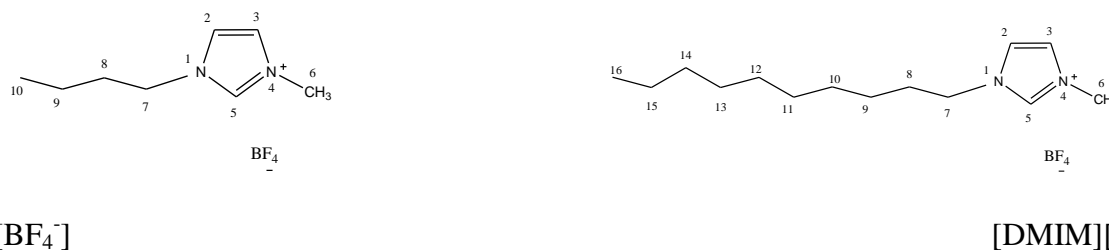
Figure 1. Schematic representation of the studied ionic liquids and the atom numbering utilized in the discussion.

Ionic liquids (ILs) are salt-like materials, which are liquids below 100 °C and possess melting points that are generally below room temperature [15, 16]. These materials possess great physicochemical properties such as excellent electrical conductivity, ability to dissolve many compounds, good thermal stability and no measurable vapour pressures. The fact that they have low or no measurable vapour pressures means that they do not release hazardous vapours into the environment, thus their classification as environmentally friendly compounds [17, 18]. The present investigation focuses on the use of imidazolium based ionic liquids as corrosion inhibitors for zinc metal in acidic medium using gravimetric methods and quantum chemical studies. Imidazolium based ionic liquids contain some nitrogen heteroatoms and an aromatic imidazole ring which act as major adsorption centers. Studies indicate that imidazolium based ionic liquids shows appreciable inhibition

efficiencies for many different metals in acidic environments [19-22]. Figure 1 shows the molecular structures of the two imidazolium based ionic liquids utilised in this investigation.

2. EXPERIMENTAL

2.1. Zinc specimens

Zinc specimens of dimensions 3.0 cm × 4.0 cm were thoroughly prepared before all the experimental measurements were done. Emery papers of various grades were used to abrade the specimens, which were then washed with distilled water, followed by acetone, and consequently left to air-dry overnight. When the drying process was completed, specimens were stored in desiccators prior to their use in all experimental measurements.

2.2. Corrosion inhibitors

The utilised ionic liquids, that is, 1-butyl-3-methylimidazolium tetrafluoroborate [BMIM][BF$_4^-$] and 1-decyl-3-methylimidazolium tetrafluoroborate [DMIM][BF$_4^-$] ionic liquids, were acquired from Sigma Aldrich Chemicals and utilised without any further purification. These are two related corrosion inhibitors originating from the same class, that is, they are composed of imidazolium cation and tetrafluoroborate anion. The only discrepancy existing between them is the alkyl chain length as depicted in figure 1.

2.3. Solutions

The corrosive medium of 1.0 M HCl was prepared through a dilution of a 32% HCl Merck Analytical grade by using appropriate amount of distilled water. A 1000 ppm stock solution of corrosion inhibitors was prepared by using appropriate amount of distilled water to facilitate the dilution of the concentrated ionic liquid. Different concentrations of corrosion inhibitors (100 - 500 ppm) were prepared through a dilution of a 1000 ppm stock solution using appropriate amounts of distilled water.

2.4. Weight loss measurements

The simplicity and reliability character traits of the weight loss method confirms it as the prime method of choice for corrosion inhibition studies as many researchers opt to utilize it [23, 24]. Weight loss experiments were conducted at 30°C, 40°C and 50°C by completely immersing zinc specimens in corrosive 1.0 M HCl solutions without and with different concentrations of corrosion inhibitors. A total immersion time of 15 h was recorded. From the weight loss measurements, parameters such as

percentage inhibition efficiency (%IE), surface coverage (θ) and corrosion rates (ρ) were calculated by making use of the equations 1-3 given below [23, 24];

$$\theta = \frac{W_2 - W_1}{W_2}$$ (1)

$$\% IE = \left(\frac{W_2 - W_1}{W_2} \right) \times 100$$ (2)

where W_1 is the weight loss in grams of zinc metal in the presence of inhibitor molecule and W_2 is the weight loss in grams of the zinc metal in the absence of inhibitor molecule.

$$\rho = \frac{\Delta W}{St}$$ (3)

where ΔW is the average weight loss of zinc metal in (g), S is the surface area of zinc metal in (cm^2) and t is the total immersion time in (s). The overall unit of corrosion rate is expressed in (g.cm^{-2}.h^{-1}).

2.5. Computational details

The quantum chemical studies were done in vacuo. Various quantum chemical parameters such the dipole moment, highest occupied molecular orbital (HOMO), the lowest unoccupied molecular orbital (LUMO), partial atomic charges, etc., were calculated and utilized to elucidate the reactive centers of the molecules and the selective centers of the molecule.

All Geometry optimizations were performed using density functional theory (DFT) with the Becke's Three Parameter Hybrid Functional using the Lee-Yang-Parr correlation functional theory (B3LYP, [25]) and using the 6-311++G(d,p) basis set. The DFT method is widely utilized in the analysis of the characteristics of the inhibitor/metal surface mechanisms and in the description of the structure nature of the inhibitor on the corrosion process [26]. DFT/B3LYP is highly recommended for the understanding of chemical reactivity and selectivity parameters including the HOMO and the LUMO densities and related properties such as polarizability, hardness (η) and electronegativity [27], electron affinity (EA) and ionization potential (IP).

All geometry optimization in vacuo were done by using the Spartan 10 V1.01 program [28]. Schematic structures were drawn using the ChemOffice package in the UltraChem 2010 version while optimized structures were drawn using the Spartan 10 V1.01 program.

3. RESULTS AND DISCUSSION

3.1. Weight loss measurements:

The values of percentage inhibition efficiency (%IE) and corrosion rate (ρ) for zinc in 1.0 M HCl at 30°C, 40°C and 50°C without and with ionic liquids are shown in table 1. The inhibition

efficiency of the ionic liquids is dependent on the temperature and concentration. The maximum inhibition efficiencies of 55.72% and 85.24% for [BMIM][BF$_4^-$] and [DMIM][BF$_4^-$], respectively is achieved at low temperatures of 30°C and maximum concentration of 500 ppm.

Table 1. Corrosion parameters obtained from weight loss of zinc in 1.0 M HCl without and with different concentrations of ionic liquids at different temperatures.

Inhibitor	Inhibitor Conc. (ppm)	Temperature					
		30°C		40°C		50°C	
		%IE	ρ (g.cm^{-2}.h^{-1})	%IE	ρ (g.cm^{-2}.h^{-1})	%IE	ρ (g.cm^{-2}.h^{-1})
	0.0	-	0.00332	-	0.00388	-	0.00615
[BMIM][BF$_4^-$]	100	49.10	0.00169	20.10	0.00310	13.17	0.00534
	200	49.70	0.00167	25.00	0.00291	16.59	0.00513
	300	53.61	0.00154	28.35	0.00278	18.70	0.00500
	400	54.52	0.00154	32.99	0.00260	19.67	0.00494
	500	55.72	0.00147	36.34	0.00247	20.65	0.00488
[DMIM][BF$_4^-$]	100	75.30	0.00082	62.37	0.00146	28.78	0.00438
	200	82.23	0.00059	71.39	0.00111	47.97	0.00320
	300	83.73	0.00054	80.15	0.00077	59.19	0.00251
	400	84.04	0.00053	81.44	0.00072	63.74	0.00223
	500	85.24	0.00049	83.76	0.00063	70.57	0.00181

Table 1 suggests that the efficiency of the ionic liquids (ILs) under this study is at its maximum at 30°C and 500 ppm for both ionic liquids utilised. At these conditions, the efficiency of [BMIM][BF$_4^-$] ranges between 45-60% while [DMIM][BF$_4^-$] has efficiencies between 75-85%. At the maximum temperature of 50°C and 500 ppm concentration of ILs, the observed ranges of efficiency are 13.2-20.7% and 28.8-70.6% for [BMIM][BF$_4^-$] and [BMIM][BF$_4^-$], respectively. The concentration of the ILs has a noticeable effect in that the concentration of the ILs increases with the inhibition efficiency.

The rate of zinc corrosion is observed to be higher in the absence of corrosion inhibitors than in their presence, and further increases with increasing temperatures. As shown in table 1, the rate of zinc corrosion is 0.00332 g.cm^{-2}.h^{-1}, 0.00388 g.cm^{-2}.h^{-1} and 0.00615 g.cm^{-2}.h^{-1} at 30°C, 40°C and 50°C, respectively, without the introduction of corrosion inhibitors. The rate of zinc corrosion decreases as the IL inhibitor concentration increases. These results show that increasing IL alkyl chain decreases the corrosion rate significantly.

3.2. Adsorption isotherm and thermodynamic parameters:

Table 2. Adsorption parameters derived from the Langmuir adsorption isotherm.

Name of inhibitor	Temperature, T/(K)	Slope	R^2	K_{ads}/(M^{-1})	ΔG^o_{ads}/($KJmol^{-1}$)
[BMIM][BF$_4$]	303	1.72	0.99	5159.96	-31.66
	313	2.17	0.97	668.45	-27.38
	323	4.15	0.99	629.33	-28.09
[DMIM][BF$_4$]	303	1.14	0.99	17950.09	-34.79
	313	1.08	0.99	5577.24	-32.91
	323	0.93	0.99	1283.20	-30.01

The mechanism followed during the adsorption process between the metal surface and the inhibitor can be evaluated through adsorption isotherms. The adsorption of the inhibitor depends largely on the charge of the metal, the nature of the chemical structure of the organic product and the type of electrolyte [29]. Adsorption isotherms for the present study have been achieved by fitting the best linear curve between concentration of the inhibitor and surface coverage. The adsorption isotherm with the maximum regression coefficients R^2 was used to calculate thermodynamic parameters pertaining to inhibitor adsorption of the inhibitor. The attempt included Temkin, Langmuir, Freundlich, Frumkin and Flory-Huggins adsorption isotherms. The best linear relationship was attained using Langmuir adsorption isotherm. The values of R^2 and slopes for the ILs inhibitors are recorded in table 2. Langmuir adsorption isotherm relates the concentration of the inhibitor and the surface coverage according to equation 4 [30]:

$$\frac{\theta}{1-\theta} = K_{ads}C_{inh} \tag{4}$$

This equation can also be rearranged into a linear form as shown in equation 5:

$$\frac{C_{inh}}{\theta} = \frac{1}{K_{ads}} + C_{ads} \tag{5}$$

where, C_{inh} is the concentration of the inhibitor, θ in the degree of surface coverage and K_{ads} is the equilibrium constant of the adsorption process. Large values of K_{ads} are associated with a more efficient process of adsorption. From equation 5 above it is clear that the plot of C_{inh}/θ against C_{inh} will give a straight line with the intercept being the inverse of K_{ads}. The plots of Langmuir adsorption isotherms are shown in figures 2.

The values of the slope obtained from the Langmuir regression line in the table 2 indicate the type of layer formed on the zinc metal surface by the adsorbed inhibitor. The closeness of the slope to unity signifies a monolayer formation [31, 32]. [BMIM][BF$_4$] has slope value of 1.72, 2.17 and 4.15,

these values imply that a multilayer was formed on the zinc metal surface. Increasing the alkyl chain on the imidazolium ring reduced the slopes and shifted them close to unity as shown by the values obtained for [DMIM][BF$_4$.

The obtained values of K_{ads} are related to the standard free energy of adsorption (ΔG^o_{ads}) according to the expression in equation 6 [33]:
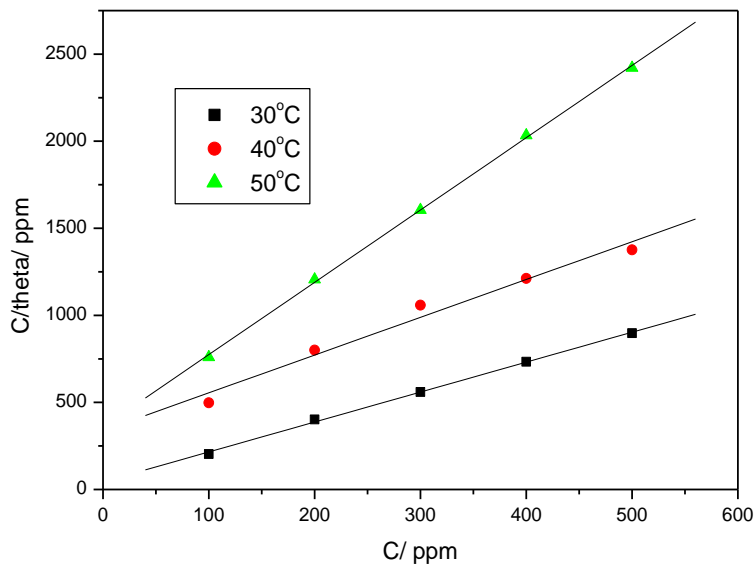
A
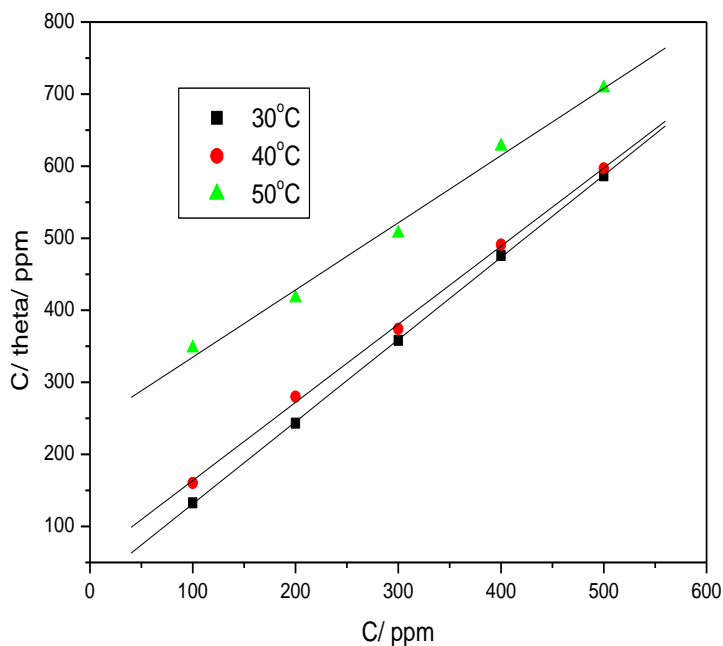
B

Figure 2. Langmuir adsorption isotherm plots for the adsorption of (A) [BMIM][BF$_4$] and (B) [DMIM][BF$_4$] on the surface of zinc metal at 30, 40, and 50°C.

$$K_{ads} = \frac{1}{55.5} \exp\left[\frac{-\Delta G^{o}{}_{ads}}{RT}\right] \qquad (6)$$

Equation 6 can also rearrange to:

$$\Delta G^{o}{}_{ads} = -2.303RT \log(55.5K_{ads}) \qquad (7)$$

where, $\Delta G^{o}{}_{ads}$ is the standard Gibbs free energy of adsorption, the value 55.5 represents the molar concentration of water in solution, T is the absolute temperature and K_{ads} is the equilibrium constant for the adsorption process. Literature suggests that the values of $\Delta G^{o}{}_{ads}$ varying between -40 KJmol^{-1} and above are associated with the sharing or transfer of an electron from the adsorbate to the surface of the substrate to form a coordinate type of bond, chemisorption (chemical adsorption mechanism) while those that are -20 KJmol^{-1} and lower indicate physisorption (physical adsorption mechanism) [34-37]. Physical adsorption occurs by weak van der Waals type of forces, no bond formed between adsorbate and substrate surface. The negative values of $\Delta G^{o}{}_{ads}$ indicate the stability of the adsorbed layer on the metal surface and spontaneity of the adsorption process while positive values symbolize a non-spontaneous adsorption process [38, 39]. Table 2 shows the values of $\Delta G^{o}{}_{ads}$, which are, all negative meaning that the adsorption process of the inhibitors on the zinc metal surface was spontaneous. All of the values of $\Delta G^{o}{}_{ads}$ are within the range of -20 KJmol^{-1} and -40 KJmol^{-1} thus both physisorption and chemisorption processes took place although predominantly physisorption.

*3.3. Effect of temperature: kinetic and thermodynamic parameters*
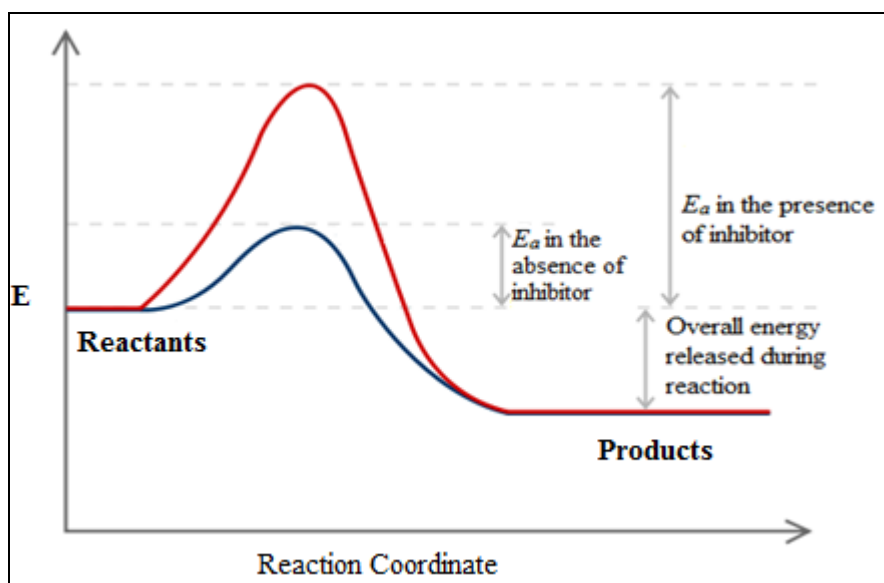
Figure 3. An illustration of the activation energy for the uninhibited and inhibited corrosion processes.

The increase in temperature generally increases the rate of corrosion [40, 41]. In all reactions, there is that minimum amount of energy that is required by the reactants to form products, such as rust

in the present investigation. This amount of energy barrier is known as the activation energy (E_a). Lower activation energies leads to high metal dissolution whereas high activation energies are associated with slow metal dissolutions as illustrated in figure 3.
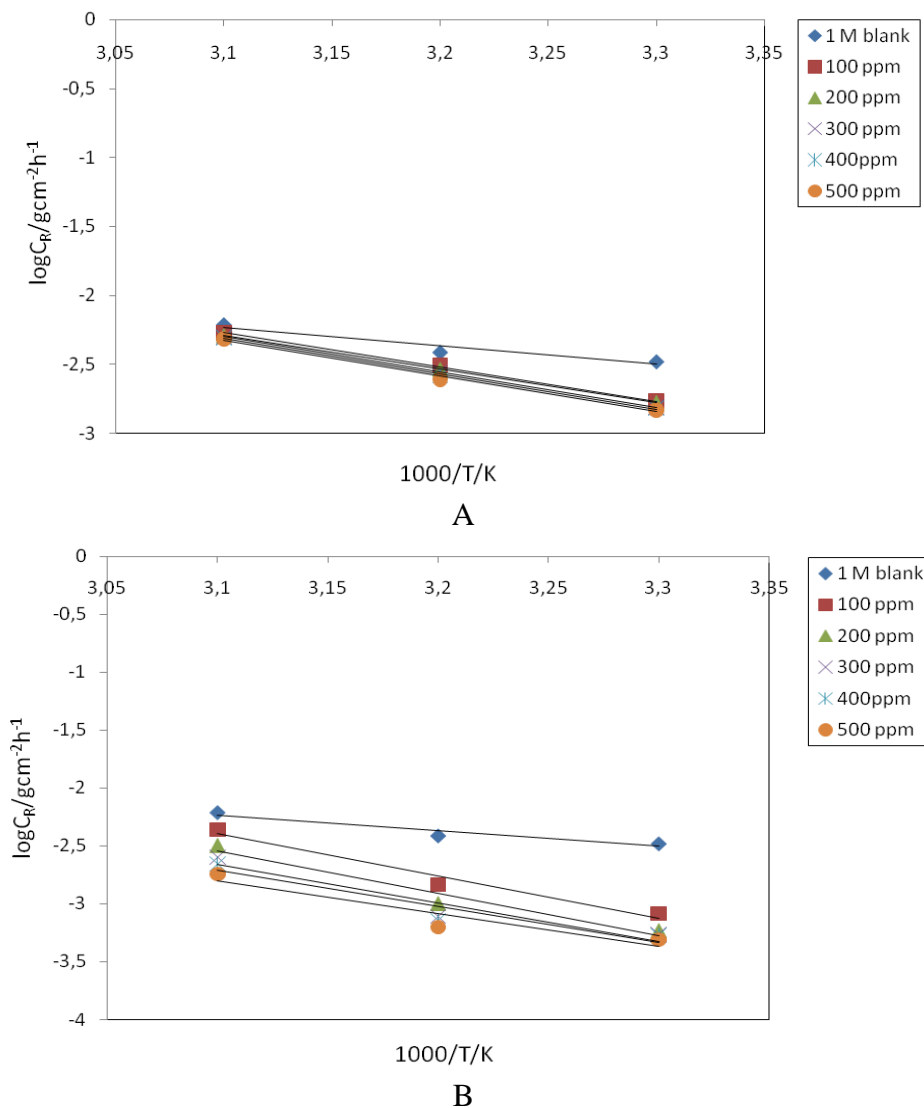
Figure 4. The plot of $\log(C_R)$ versus *1/T* (Arrhenius plot for zinc metal corrosion in 1 M HCl in the absence and presence of different concentrations of :(A) [BMIM][BF$_4$] and (B) [DMIM][BF$_4$].

The effect of temperature on the adsorption behaviour and activation energy parameters of the corrosion process can be evaluated using the Arrhenius equation below [42]:

$$K = Ae^{-\frac{E_a}{R}\left(\frac{1}{T}\right)} \qquad (8)$$

This equation can also be expressed in the logarithms form as:

$$\log C_R = \log A - \frac{E_a}{2.303RT}$$

(9)

where, C_R is the corrosion rate, E_a is the apparent activation energy, R is the molar gas constant (8.314 $JK^{-1}mol^{-1}$), T is the absolute temperature and A is the frequency factor. The plots of $\log(C_R)$ against 1/T for zinc in 1 M HCl in the absence and presence of different concentrations of [BMIM][BF$_4$] and [DMIM][BF$_4$] are shown in the figure 4.

From the Arrhenius equation and plots, values of activation energy can be obtained using the slopes and intercepts of the regression lines.

The process of adsorption between the metal surface and the inhibitor can sometimes be an exothermic process where the heat is given off, although in some cases, endothermic process is encountered. The higher activation energy values indicate physical adsorption mechanism while the lower ones attribute for chemical adsorption mechanism [43]. Eddy et al have reported that the values of activation energy less than 80 $KJmol^{-1}$ represent physical adsorption [44].

The effect of temperature on the inhibition efficiency of the of zinc metals surface can also be investigated by determining the entropy and enthalpy of activation. Negative values of entropy indicates that the transition state in the region of activated complex has a more rigid structure (favourable) while the positive once shows that the system has become more disordered (unfavourable) [45]. Generally, a positive values of enthalpy of activation *(ΔH*)* resemble an endothermic nature of the zinc dissolution process while the negative ones reveal that the adsorption of the inhibitor molecules is an exothermic process [46].

Transition state equation relates the corrosion rate and temperature as:

$$C_R = \frac{K_B}{h} \exp\left(\frac{\Delta S^*}{R}\right) \exp\left(\frac{-\Delta H^*}{RT}\right)$$
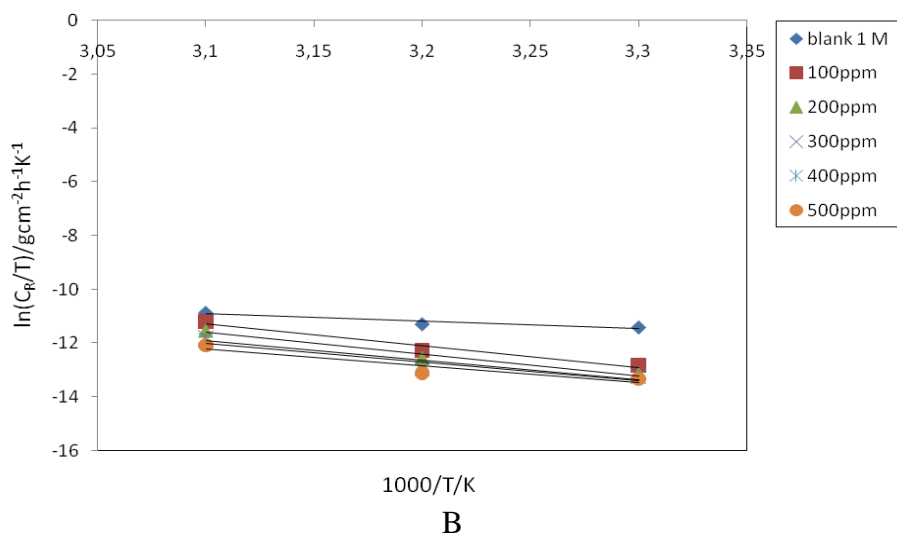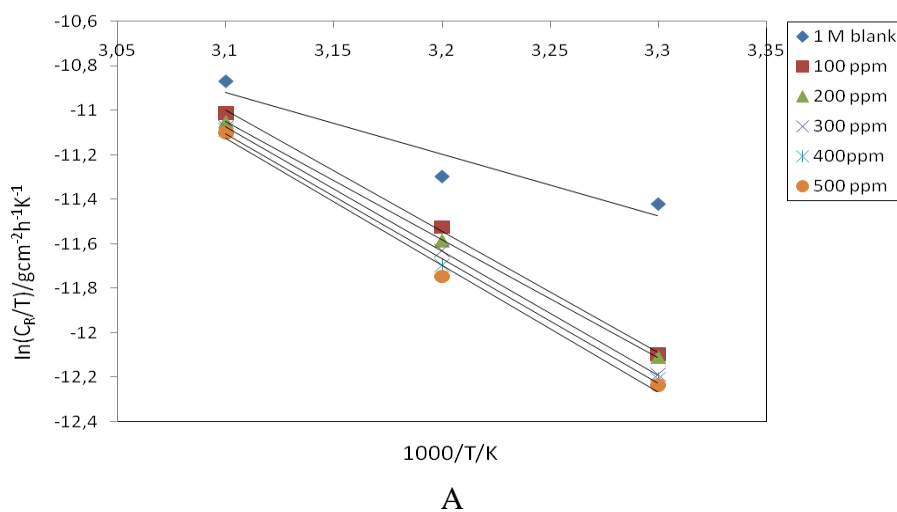
(10)

This equation can also be expressed as:

$$\ln\left(\frac{C_R}{T}\right) = \ln\left(\frac{K_B}{h}\right) + \frac{\Delta S^*}{R} - \frac{\Delta H^*}{RT}$$

(11)

where, ΔS^* is the apparent entropy of activation, ΔH^* is the apparent enthalpy of activation, k_B is the Boltzmann's constant, C_R is the corrosion rate and h is the Plank's constant. The transition state plots of $\ln(C_R/T)$ versus 1/T (figure 5) were utilised to calculate the values of ΔS^* and ΔH^*. These values are recorded in table 3.

Table 3. The values of activation energy E_a, enthalpy of activation ΔH^*, and entropy of activation ΔS^* for zinc metal in the absence and presence of different inhibitors at different concentrations.

| Name of inhibitor	Concentration of inhibitor (ppm)	(E_a/KJmol^{-1})	(ΔH^*/KJmol^{-1})	(ΔS^*/JK^{-1}mol^{-1})
-	-	25.66	22.99	-217.06
[BMIM][BF$_4$]	100	47.87	45.19	-148.91
	200	46.62	44.02	-152.95
	300	48.92	46.31	-146.05
	400	49.30	46.59	-145.39
	500	49.88	47.22	-143.65
[DMIM][BF$_4$]	100	69.59	66.97	-83.84
	200	70.27	69.13	-84.26
	300	63.95	61.23	-106.67
	400	59.74	57.08	-120.54
	500	54.28	51.67	-139.00

A

B

Figure 5. Transition state plots at different concentrations of: (A) [BMIM][BF$_4$] and (B) [DMIM][BF$_4$].

From table 3, the value of E_a for the blank was found to be 25.66 KJmol^{-1}. Introducing the inhibitors in the solution increased all values of activation energy barriers hence the rate of metals dissolution was decreased. At 100 ppm of [BMIM][BF$_4$] the value of activation increased to 47.87 KJmol^{-1} and 300 ppm and 500 ppm the values increased further to 48.92 KJmol^{-1} and 49.88 KJmol^{-1}, compared to that of the blank. This observation is illustrated in figure 3. A noticeable effect of increasing inhibitor concentration is revealed by the amount of the activation energy, wherein the activation energy increases with the increasing inhibitor concentration. This trend reinforce the fact that high activation energies will inhibit the rate of metal dissolution and this also correlate with the amount of surface coverage reported above in this study. The activation energies for the uninhibited and two inhibited processes follow the order [DMIM][BF$_4$] > [BMIM][BF$_4$] > [Blank]. Ostovari A et al reported enthalpy values up to 41.86 KJmol^{-1} are attributed to physisorption while those that are around 100 KJmol^{-1} or more are attributed to chemisorption [47]. The obtained values of enthalpy in table 3 are all positive. The fact that the inhibited processes have higher values of activation energy than that of uninhibited process is an evidence of adsorption process between the inhibitor and the metal surface. The reported enthalpy values range between 41.86 KJmol^{-1} and 100 KJmol^{-1}, indicating a mixed type adsorption process.

Table 3 shows negative values entropy of activation whereby the highest entropy value is negative 217.06 JK^{-1}mol^{-1} corresponding to the uninhibited process. The values of ΔS* were lower for the solution with inhibitor than that of the solution without inhibitor. The shift of ΔS* to less negative values in the presence of the inhibitor decreases the disorder. At 100 ppm concentration of [BMIM][BF$_4$] inhibitor, -148.19 JK^{-1}mol^{-1} was obtained and increasing the concentration to 500 ppm reduced further the entropy value to -143.65 JK^{-1}mol^{-1}. A significant decrease of the entropy values is observed with the IL of high steric hindrance [DMIM][BF$_4$] where -83.84 JK^{-1}mol^{-1} was obtained at a low concentration of 100 ppm. This value signifies that [DMIM][BF$_4$] inhibitor best inhibits the rate of zinc dissolution even at lower inhibitor concentrations.

3.4. Quantum chemical results

Optimized geometry   LUMO   HOMO
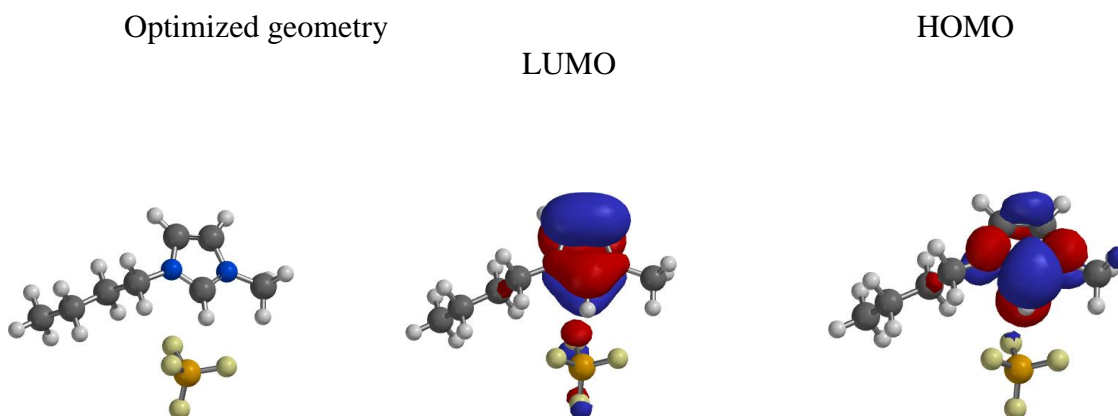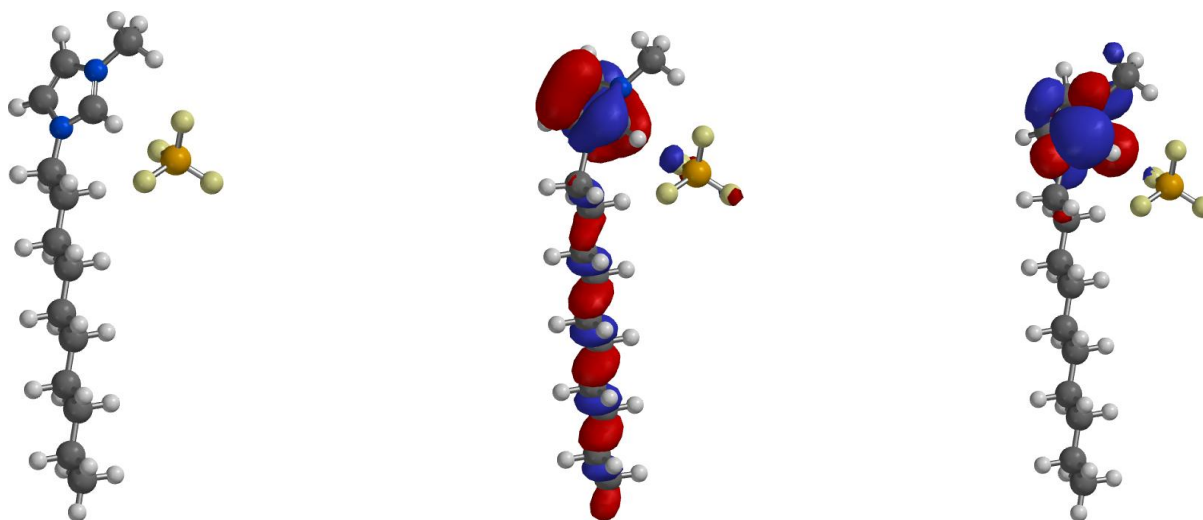
Figure 6. The optimised geometries and the corresponding HOMO and LUMO for the studied ionic liquids, B3LYP/6-311++G(d,p) results.

The optimized geometries of the two imidazolium-based ionic liquids are shown in figure 6 together with the HOMO and the LUMO of each structure. The HOMO density of $[BMIM][BF_4^-]$ is exclusively localized on the cation, above and below the benzene ring, what suggest that on interaction with the metal surface, the inhibitor binds to the metal by donating electrons from the benzene ring. The HOMO density of $[DMIM][BF_4^-]$ is delocalised across the benzene ring and on the long alkyl chain. These results indicate that $[DMIM][BF_4^-]$ has more site for donating electrons to the metal surface than $[BMIM][BF_4^-]$ which in turn suggests that $[DMIM][BF_4^-]$ would have greater tendency to bind on the metal surface than $[BMIM][BF_4^-]$. This prediction is in good agreement with the experimental findings that show that the inhibition efficiency of $[DMIM][BF_4^-]$ is greater than that of $[BMIM][BF_4^-]$.

Table 4. The molecular properties for ionic liquids. B3LYP/6-31G(d,p) results *in vacuo*. The experimental percentage inhibitor efficiency (%IE) is included in the last row of each table for comparison purpose.

	$[BMIM][BF_4^-]$	$[DMIM][BF_4^-]$
E_{HOMO} (eV)	-8.27	-8.23
E_{LUMO} (eV)	-1.40	-1.39
ΔE (eV)	6.87	6.84
Dipole moment (Debye)	12.37	12.21

Other molecular quantum chemical parameters related to the reactivity of molecules are reported in table 4 and include the energy of the highest occupied molecular orbital (E_{HOMO}), energy of the lowest unoccupied molecular orbital (E_{LUMO}), the energy gap ($E_{LUMO-HOMO}$, ΔE) and dipole moment (μ). E_{HOMO} is often associated with the electron donating ability of a molecule [48] and a higher E_{HOMO} value indicates higher tendency of the molecule to donate electron(s) to an electron deficient species.

The results reported in table 4 show that E_{HOMO} for the two inhibitors is such that $[DMIM][BF_4^-] >$ $[BMIM][BF_4^-]$. Therefore $[DMIM][BF_4^-]$ has the highest tendency to donate electrons to the surface of the metal and therefore would have the highest tendency to adsorb onto the metal surface; this result is in agreement with the analysis of the HOMO density and with experimental findings.

ΔE informs about the reactivity of a molecule towards other chemical species. Molecules with large value of ΔE are highly stable while molecules with small values of ΔE have a high reactivity. The data reported in table 4 show $[DMIM][BF_4^-]$ has the smaller ΔE value than $[BMIM][BF_4^-]$ and therefore would corresponding to the most reactive compound. This means that $[DMIM][BF_4^-]$ has greate tendecy to react/interact with the metal surface leading to high inhibition efficiency. Since $[DMIM][BF_4^-]$ has the highest tendency to donate electrons and also the highest tendency to react with the metal surface it is reasonable to infer that it would have the highest tendency to bind on the metal surface, what is in agreement with the experimental observation that $[DMIM][BF_4^-]$ is the most efficient corrosion inhibitor.

The dipole moment informs about the polarity of the compounds and also informs about the reactivity of molecules. In the study of corrosion inhibitors, the dipole moment does not always show univocal trend; several reserach works have reported that the dipole moment increases with increase in the inhibition efficiencies of the inhibitors [49]; other research works have shown that dipole moment decreases with increase in the inhibition efficiencies of the inhibitors [50]; there are also research works that show that the dipole moment does not have good correlation with the inhibition efficiencies of the inhibitors [51]. A comparison of the trend in the dipole moment of the studied ionic liquids and the trend in their corrosion inhibition efficiecies shows that a smaller dipole moment corresponds to higher inhibition efficiency.

Table 5. Mulliken atomic charges and the condensed Fukui functions on the selected atom for the studied ionic liquids. B3LYP/6-311++G(d,p) results *in vacuo*.

atom	[BMIM][BF$_4^-$]			[DMIM][BF$_4^-$]		
	Mulliken charge	$f^+ = q_{(N+1)} - q_N$	$f^- = q_N - q_{(N-1)}$	Mulliken charge	$f^+ = q_{(N+1)} - q_N$	$f^- = q_N - q_{(N-1)}$
N1	0.126	-0.063	0.007	0.172	-0.054	0.006
C2	-0.043	0.616	-0.099	-0.015	0.522	-0.047
C3	-0.122	0.831	-0.106	-0.137	0.725	-0.061
N4	0.102	-0.087	-0.003	0.117	-0.069	0.002
C5	-0.433	0.667	-0.037	-0.437	0.596	-0.027
C6	-0.263	0.670	-0.005	-0.257	0.586	-0.001
C7	-0.234	0.291	0.015	-0.360	0.278	0.003
C8	-0.242	-0.097	0.003	-0.371	-0.099	-0.004
C9	-0.180	0.157	0.024	-0.159	0.069	0.014
C10	-0.593	0.026	-0.027	-0.298	0.087	-0.003
C11				-0.158	0.011	0.009
C12				-0.278	0.015	0.002
C13				-0.222	0.056	0.001
C14				-0.135	0.033	0.007
C15				-0.163	-0.039	0.011
C16				-0.555	0.230	-0.024

Among the parameters that inform about the selectivity of the molecule include the partial atomic charges and the condensed Fukui functions. The partial atomic charges on the atoms have proven to be another useful quantum chemical parameter in the study of corrosion inhibitors [52, 53]. Table 5 reports the partial atomic charges for the studied ionic liquids as well as the corresponding Fukui functions. The charges are reported for only the cationic moiety because there are minimal changes in the charges on the anionic moiety. The highest negative charge is on last C atom in the alkyl chain. The C5 atom has the highest negative charge in the imidazolium ring. In comparing the two compounds, we note that the charge on the C5 is higher for [DMIM][BF_4^-] than for [BMIM][BF_4^-]. Moreover, since [DMIM][BF_4^-] has a longer alkyl chain than [BMIM][BF_4^-], it has more sites that have high negative charge than [BMIM][BF_4^-]. These suggest that [DMIM][BF_4^-] has more sites that can interact with the metal surface than [BMIM][BF_4^-], what confirms the HOMO analysis. The more negative the atomic charge of the adsorbed centre is, the easier it is for the atom to donate its electrons [54]. It is therefore reasonable to anticipate that [DMIM][BF_4^-] would interact more with the metal surface than [BMIM][BF_4^-], what is in agreement with the HOMO density analysis.

The condensed Fukui functions provide information about the atoms in a molecule that have a tendency to either donate (nucleophilic character) or accept (electrophilic character) an electron or pair of electrons. The nucleophilic and electrophilic Fukui functions can be calculated using the finite difference approximation as follows [55]:

$$f^+ = q_{(N+1)} - q_N \tag{12}$$
$$f^- = q_N - q_{(N-1)} \tag{13}$$

where $q_{(N+1)}$, q and $q_{(N-1)}$ are the charges of the atoms on the systems with *N+1*, *N* and *N−1* electrons respectively. The preferred site for nucleophilic attack is the atom or region in the molecule where the value of f^+ is the highest while the site for electrophilic attack is the atom/region in the molecule where the value of f^- is the highest. In the two ionic liquid systems investigated in this work, it is evident that both the preferred sites for the nucleophilic and electrophilic attacks are in the imidazolium ring.

4. CONCLUSIONS

The work presented the experimental and DFT studies on selected ionic liquids to investigate the influence of the substituent groups on the ability of the ionic liquids to inhibit Zinc surface corrosion. The results show that:

- Inhibition efficiency increases with the increase in the length of the R chain.
- The inhibition efficiency increases and corrosion rate decreases with increase of concentration, with the maximum %IE of 85.24 for [DMIM][BF_4^-] at 500 ppm.

- Weight loss and computational studies results are in good agreement and show that the two ionic liquids are good corrosion inhibitors for zinc corrosion in 1.0 M HCl solutions and their inhibition efficiency follows the order: $[DMIM][BF_4^-] > [BMIM][BF_4^-]$.
- The adsorption of ILs on zinc metal surface adopted the Langmuir adsorption isotherm model.
- The values of the activation energy and enthalpy of activation indicate a spontaneous adsorption process and follow the physical adsorption mechanism.
- The increase in the inhibition efficiency with the increase in the length of the R chain maybe related to the increase in the hydrophobic nature of the molecule. The higher the hydrophobic nature the lesser is the tendency of the molecule to remain in solution, what means that its interaction with the metal surface is increased.
- B3LYP/6-311++G(d,p) has been utilised to identify and compare the reactive sites for the two ionic liquid.

References

1. Y. Furukawa, J. Kim, J. Watkins, R.T. Wilkin, *Environ. Sci. Technol.,* 36 (2002) 5469.
2. A.M. Badiea, K.N. Mohana, *J. Mater. Engr. Perform.,* 18 (2008) 1265.
3. N.O. Obi-Egbedi, I.B. Obot, *Arab. J. Chem.,* 5 (2012) 122.
4. M.A. Quraishi, M.Z.A. Rafiguee, S. Khan, N. Saxena, *J. Appl. Electrochem.,* 37 (2007) 1154.
5. E.E. Ebenso, I.B. Obot, L.C. Murulana, *Int. J. Electrochem. Sci.,* 5 (2010) 1575.
6. A.K. Singh, M.A. Quraishi, *J. Mater. Environ. Sci.,* 1 (2010) 102.
7. K.R. Ansari, M.A. Quraishi, A. Singh, *Corros. Sci.,*7 (2014) 5.
8. R.A. Prabhu, T.V. Venkatesha, A.V. Shanbhag, B.M. Praveen, G.M. Kulkarni, R.G. Kalkhambkar, *Mater. Chem. Phys.,* 108 (2008) 283.
9. N. O. Obi-Egbedi, K.E. Essien, IB. Obot, E.E. Ebenso, *Int. J. Electrochem. Sci.,* 6 (2011) 915.
10. S.K. Shukla, E.E. Ebenso, *Int. J. Electrochem. Sci.,* 6 (2011) 3274.
11. E.E. Ebenso, T. Arslan, F. Kandermirli, N. Caner, I. Love. *Int. J. Quantum. Chem.,* 110 (2010) 1005.
12. I B. Obot, N.O. Obi-Egbedi, S.A. Umoren, E.E. Ebenso, *Chem. Eng. Comm.,* 198 (2011) 713.
13. G. Avci, *Colloids. Surf. A: Physicochem. Eng. Aspects.,* 317 (208) 733.
14. P.B. Raja, M.G. Sethuraman, *Mater. Letts.,* 62 (2008) 113.
15. K.E. Jonson, *Electrochem. Soc. Interf.,* (2007) 38.
16. J.S. Wikes, *Green. Chem.,* 4 (2002) 73.
17. Y.R. Jorapur, D.Y. Chi, *Bull. Korean. Chem. Soc.,* 27 (2006) 345.
18. G. Singh, A. Kumar, *Indian. J. Chem.*, 47A (2008) 499.
19. L.C. Murulana, A.K. Singh, S.K. Shukla, M.M. Kabanda, E.E. Ebenso, *Ind. Eng. Chem. Res.,* 51 (2012) 13284.
20. S.K. Shukla, L.C. Murulana, E.E. Ebenso, *Int. J. Electrochem. Sci.,* 6 (2011) 4288.
21. M. Uerdingen, C. Treber, M. Balser, G. Schimitt, C. Werner, *Green. Chem.,* 7 (2005)322.

22. M. Hasib-ur-Rahman, F. Larachi, *Ind. Eng. Chem. Res.,* 52 (2013) 17682.
23. E.F. Olasehinde, A.S. Adesina, E.O. Fehintola, B.M. Badmus, A.D. Aderibidge, *J. Appl. Chem.,* 2 (2012) 16.
24. H. Ashassi-Sorkhabi, M. Es'haghi, *Mater. Chem. Phys.,* 114 (2009) 268.
25. A. D. Becke, *J. Chem. Phys.,* 98 (1993) 5648.
26. A.Zarrouk, H. Zarrok, R. Salghi, B. Hammouti, F. Bentiss, R. Touir, M. Bouachrine, *J. Mater. Environ. Sci.* 4 (2013) 179.
27. B. Hmamou, R. Salghi, A. Zarrouk, M. R. Aouad, O. Benali, H. Zarrok, M. Messali, B. Hammouti, E.E. Ebenso, M. Bouachrine, M.M. Kabanda. *Ind. Eng. Chem. Res.*, 52 (2013) 14327.
28. Spartan,10 Wavefunction, Inc. Irvine, CA: Y. Shao, L.F. Molnar, Y. Jung, J. Kussmann, C. Ochsenfeld, S.T. Brown, A.T.B. Gilbert, L.V. Slipehenko, S.V. Levehenko, D. P. O'Neill, R.A. DiStasio Jr., R.C. Lochan, T.Wang, G.J.O. Beran, N.A. Besley, J.M. Herbert, C.Y. Lin, T. Van Voorhis, S.H. Chien, A. Sodt, R.P. Steele, V.A. Rassolov, P.E. Maslen, P.P. Korambath, R.D. Adamson, B. Austin, J. Baker, E.F.C. Byrd, H. Dachsel, R.J. Doerksen, A. Dreuw, B.D. Dunietz, A.D. Dutoi, T.R. Furlani, S.R. Gwaltney, A. Heyden, S. Hirata, C.P. Hsu, G. Kedziora, R.Z. Khalliulin, P.Klunzinger, A.M. Lee, M.S. Lee, W.Z. Liang, I.Lotan, N. Nair, B.Peters, E.I. Proynov, P.A. Pieniazek, Y.M. Rhee, J. Ritchie, E. Rosta, C.D. Sherrill, A.C. Simmonett, J.E. Subotnik, H.L. Woodcock III, W. Zhang, A.T. Bell, A.K. Chakraborty, D.M. Chipman, F.J. Keil, A. Warshel, W.J. Hehre, H.F. Schaefer, J. Kong, A.I. krylov, P.M.W. Gill and M. Head-Gordon, *Phys. Chem. Chem. Phys.,* 8 (2010) 3172.
29. Y. Tang, F. Zhang, S. Hu, Z. Cao, Z. Wu, W. Jing, *Corros. Sci.,* 74 (2013) 276.
30. F. Zhang, Y. Tang, Z. Cao, W. Jing, Z. Wu, Y. Chen, *Corros. Sci.,* 61 (2012) 6.
31. L. Fragoza-Mar, O. Olivares-Xometl, M.A. Dominguez-Aguilar, E.A. Flores, P. Arellanes-Lozada, F. Jimenez-Cruz, *Corros. Sci.,* 74 (2013) 276.
32. N.V. Likhanova, M.A. Dominguez-Aguilar, M. Olivares-Xometl, N. Nava-Entzana, E. Arce, H. Dorantes, *Corros. Sci.,* 61 (2012) 175.
33. E.E. Ebenso, I.B. Obot, *Int. J. Electrochem. Sci.,* 5 (2010) 2024.
34. U.M. Eduok, S.A. Umoren, A.P. Udoh, *Arab. J. Chem.,* 5 (2012) 334.
35. M.J. Bahrami, S.M.A. Hosseini, P. Pilvar. *Corros. Sci.,* 52 (2010) 2797.
36. A. A. Nazeer, H.M. El-Abbasy, A.S. Fouda, *Res. Chem. Intermed.,* 39 (2013) 925.
37. Y. Abboud, B. Hammouti, A. Abourriche, A. Bennamara, H. Hannache, *Res. Chem. Intermed.,* 38 (2012) 1600.
38. A. A. Nazeer, H.M. El-Abbasy, A.S. Fouda, *J. Mater. Eng. Perform.,* 22 (2013) 6321.
39. M. Yafav, D. Behera, S. Kumar, R.R. Sinha, *Ind. Eng. Chem. Res.,* 52 (2013) 6321.
40. M.S. Morad, A.M. Kamal El- Dean, *Corros. Sci.,* 48 (2006) 3404.
41. G. Moretti, G. Quartarone, A. Tassan, A. Zingales, *Electrochimica Acta.,* 41 (1996) 1978.
42. M. Bouklah, B. Hammouti, M. Lagrenee, F. Bentis, *Corros. Sci.,* 48 (2006) 2835.
43. F. Bentis, M. Lebrini, M. Lagrenee, *Corros. Sci.,* 47 (2005) 2925.
44. N.O. Eddy, F. Awe, E.E. Ebenso, *Int. J. Electrochem. Sci.,* 5 (2010) 2003.
45. I.E. Uwah, P.C. Okafor, V.E. Ebiekpe, *Arab. J. Chem.,* 6 (2013) 290.
46. M. Kaddouri, S. Rekkab, M. Bouklah, B. Hammouti, A. Aouniti, Z. Kabouche, *Res. Chem. Intermed.,* 39 (2013) 3661.
47. A. Ostovari, S.M. Hosseinieh, M. Peikari, S.R. Shadizadeh, S.J. Hashemi, *Corros. Sci.,* 51 (2009) 1936.
48. A.K. Singh, S. Khan, A. Singh, S.M. Quraishi, M.A. Quraishi, E.E. Ebenso, *Res. Chem. Intermed.,* 39 (2013) 1205.
49. C.M. Goulart, A. Esteves-Souza, C.A. Martinez-Huitle, C.J.F Rodriguez, M.A.M Maciel, A. Echevarria, *Corros. Sci.,* 67 (2013) 286.
50. I.B. Obot, E.E. Ebenso, M.M. Kabanda, *J. Environ. Chem. Eng.*, 1 (2013) 439.

51. N.O. Obi-Egbedi., I.B. Obot., M.I. El-Khaiary., S.A. Umoren, E.E. Ebenso. *Int. J. Electrochem. Sci*., 6 (2011) 5649.
52. G. Gece, *Corros. Sci*., 50 (2008) 2981.
53. G. Gao, C. Liang. *Electrochim. Acta.,* 5 (2007) 4554.
54. A.K. Chandra, M.T. Nguyen, *Int. J. Mol. Sci., 3 (*2002) 310.
55. P. Fuentealba, P. Perez, R. Contreras, *J. Chem. Phys.,* 113 (2000) 2544.